Room Temperature Metalation of 2H-TPP Monolayer on Iron and Nickel Surfaces by Picking up Substrate Metal Atoms

Andrea Goldoni,[†,*] Carlo A. Pignedoli,[‡] Giovanni Di Santo,[†] Carla Castellarin-Cudia,[†] Elena Magnano,[§] Federica Bondino,[§] Alberto Verdini,[§] and Daniele Passerone[‡]

[†]ST-INSTM Laboratory, Sincrotrone Trieste S.C.p.A. s.s.14 km. 163.5, 34149 Trieste, Italy, [‡]Empa, Swiss Federal Laboratories for Materials Science and Technology, Nanotech@surfaces Laboratory, Ueberlandstrasse 129, CH-8600 Dübendorf, Switzerland, and [§]TASC Laboratory, Istituto Officina dei Materiali-CNR, s.s. 14 km 163,5, 34149 Trieste, Italy

ABSTRACT Here, it is demonstrated, using high-resolution X-ray spectroscopy and density functional theory calculations, that 2*H*-tetraphenyl porphyrins metalate at room temperature by incorporating a surface metal atom when a (sub)monolayer is deposited on 3d magnetic substrates, such as Fe(110) and Ni(111). The calculations demonstrate that the redox metalation reaction would be exothermic when occurring on a Ni(111) substrate with an energy gain of 0.89 eV upon embedding a Ni adatom in the macrocycle. This is a novel way to form, *via* chemical modification and supramolecular engineering, 3d-metal−organic networks on magnetic substrates with an intimate bond between the macrocycle molecular metal ion and the substrate atoms. The achievement of a complete metalation by Fe and Ni can be regarded as a test case for successful preparation of spintronic devices by means of molecular-based magnets and inorganic magnetic substrates.

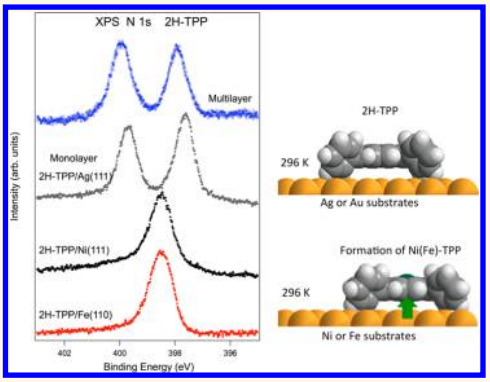

KEYWORDS: porphyrins · interfaces · X-ray spectroscopy · surface chemistry · density functional calculations

The chemical bond of adsorbates on metal surfaces is of fundamental interest in surface science and molecular electronics, where a big challenge is to engineer novel devices based on the interaction of an active nanoscale site with the surrounding medium. This is a highly appealing perspective that allows the fabrication of functional macromolecular architectures directly on a surface through surface-driven chemistry using the bottom-up approach.[1−4]

Porphyrins and similar planar molecular systems are extremely suitable for this task because they combine the self-assembling properties into ordered templates on surfaces with the presence of active sites of interaction within the molecules themselves.[5−7] Therefore, these stable and versatile π-conjugated planar metallo-organic molecules find a multitude of applications in solid state chemistry and 2D molecular engineering for opto-electronics, biological and artificial structures, chemical sensors, photovoltaic devices, or catalytic and magnetic systems.[8−12]

Porphyrins may be deposited in the submonolayer regime on single-crystal surfaces in ultrahigh vacuum (UHV) systems, and the interaction with the surface can be used to change the properties of the adsorbed molecules. Recently, it was demonstrated that metal ions can be incorporated into adsorbed free-base tetrapyrrole molecules, like porphyrins or phthalocyanines, by metal UHV evaporation. This metalation process is a redox reaction resulting in the oxidation of the metal and a reduction of the porphyrin ligand. By adding various metals *via* UHV evaporation, it is possible to metalate the free-base porphyrins at the center of the macrocycle both in monolayer and multilayer regimes.[13−21] This approach offers novel pathways to realize metallo-porphyrin compounds, low-dimensional metal−organic architectures,

* Address correspondence to andrea.goldoni@elettra.trieste.it.

Received for review September 7, 2012 and accepted November 13, 2012.

Published online 10.1021/nn304134q

and patterned surfaces, which cannot be achieved by conventional means.[22] Potentially, this route can also be employed to synthesize extremely reactive metallo-porphyrins, whose instability prevents a direct evaporation, but the presence of a surface may allow their existence. For example, unfavorable oxidation states of the metal ion may be stabilized by the interaction with the underlying surface, which can act as an electron donor. It is worth noting that some metallo-porphyrins containing Fe, Mn, Au, Rh, *etc*. ions are stabilized as free molecules by bonding the macrocycle ion to another atom, typically Cl, or functional groups, but the same metallo-porphyrins may also be stabilized on a surface by evaporating the metal ions into the free-base porphyrins (see the Supporting Information for X-ray photoemission data on Rh and Mn metalation of 2H-TPP).[7,13] As a consequence, the chemical identification of the different molecular species that can be formed on a surface/interface and of their interactions with the substrate become a major challenge. This is very important when unobvious changes in the adsorbed layer can lead to the formation of new molecular species.[23−25]

Recently, Gonzales-Moreno *et al.*[26] using a protoporphyrin, Raval and co-workers using diphenyl porphyrins and octaethyl porphyrins (OEP),[24,27] and Diller *et al.*[28] using 2*H*-tetraphenyl porphyrin (2H-TPP) have shown that metalation of porphyrins can be achived also by deposting metal-free molecules on copper surfaces just picking up substrate metal atoms and forming Cu porphyrins. In all of these Cu cases, apart from protoporphyrins on Cu(110),[26] the samples need to be annealed above 380 K to complete the redox reaction. The fact that only the simplest molecule, protoporphyrin, on Cu(110) may metalate at room temperature demonstrates that the interface interaction and, in particular, the interplay between the geometric and the electronic structures are very complex: the adsorption geometry, molecular conformation, charge, and spin states at the interface are extremely critical in determining the behavior of the system.

Here we demonstrate, using high-resolution X-ray spectroscopy and density functional theory calculations that, by depositing a (sub)monolayer of more complex molecules, like 2H-TPP, on Fe(110) and Ni(111) surfaces at room temperature, the macrocycle binds directly to an adatom of the metallic substrate that metalates the porphyrin, forming Fe-TPP and Ni-TPP, respectively.

RESULTS AND DISCUSSION

We start with the deposition of 1 ML (or sub-ML) of 2H-TPP molecules on Ni(111) and on a thin layer (15 ML) of γ-Fe(110)/Cu(110) at room temperature. Figure 1 shows the N 1s core level photoemission spectra of these monolayers compared with the spectrum of a multilayer and the spectrum of a monolayer on Ag(111).

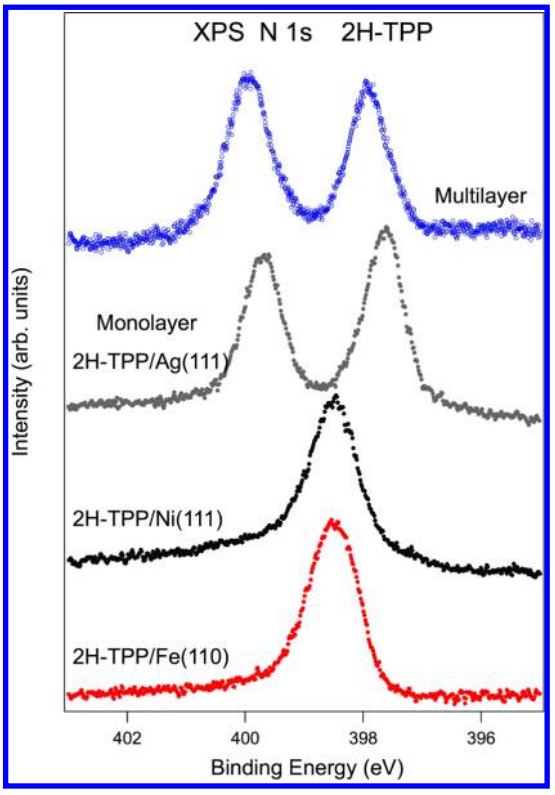

Figure 1. N 1s photoemission spectra of (from top to bottom) a 2H-TPP multilayer, monolayer on Ag(111), monolayer on Ni(111), and monolayer on Fe(110). In the latter two cases, the presence of a single N 1s peak is a fingerprint for the formation of Ni-TPP and Fe-TPP.

It is evident that while in the multilayer and monolayer on Ag(111) the N 1s spectrum is composed of two peaks, corresponding to non-equivalent iminic (397.9 and 397.6 eV, respectively) and pyrrolic (399.9 and 399.6 eV, respectively) nitrogen atoms, both in the case of Ni(111) and Fe(110) substrates, the spectra consist of one single peak (at about 398.5 eV in both cases).

These values are, within $\pm$0.1 eV, akin to other reports.[7,20,21,29] The spectra were taken just after the deposition of about 1 ML with the substrate at room temperature. Similar spectra were also measured after the formation of one monolayer obtained by sublimating the multilayer, for example, by annealing the multilayer at 570 K. The samples were carefully checked for radiation damage. In order to minimize any effects from the irradiation, the light spot was scanned over the sample and several spectra were recorded in different positions with the same results.

The presence of one single N 1s peak and its binding energy between the iminic and pyrrolic peaks is the clear confirmation that the four nitrogen atoms are now equivalent and coordinated with a metal atom. We will show that this is due to the metalation of the 2H-TPP molecules by suction of an atom from the

substrate, with subsequent formation of Fe-TPP and Ni-TPP, respectively.

Apparently withstanding the proposed process, it is well-established that, in the monolayer regime upon adsorption at room temperature, 2H-TPP exhibits a conformational adaptation with a considerable rotation of the phenyl substituents with respect to the macrocycle plane, mainly due to the steric effect of hydrogen atoms.[30] This causes the macrocycle to be at a distance d between 2.5 Å < d < 5 Å depending on the possible distortion of the macrocycle ring.[7,31] Our experimental data indicate that, even considering the large macrocycle distance, the metalation may occur, and this will be the first experimental proof of this phenomenon for a TPP at room temperature. Obviously, this does not happen on all substrates, as demonstrated by the silver and even gold cases (not shown here), although both Ag and Au form stable porphyrin complexes.

To further elucidate this observation, in Figure 2, we show the N 1s near-edge X-ray absorption fine structure (NEXAFS) spectra of the present 2H-TPP monolayer deposited on Ni(111) (black spectrum) and Fe(110) (red spectrum) compared with the spectra measured for Ni-OEP,[32] Fe-TPP,[21] and Fe-OEP-Cl[33] metallo-porphyrin monolayers on several metallic substrates and for 2H-TPP on Ag(111). As we can see, the spectra measured on Ni(111) and Fe(110) are almost identical to those of similar metallo-porphyrin molecules with Ni and Fe in the macrocycle adsorbed on other metal substrates, further pointing to the possible metalation of 2H-TPP, while for 2H-TPP deposited on Ag(111), there is a clear difference in the spectrum which is shifted to lower photon energy with the presence of two π^* transitions at 397.6 and 399.6 eV corresponding to the iminic and pyrrolic N species still present here.

Previous density functional theory (DFT) calculations of the metalation process for the first row d-metals predict increasing activation barriers in the following order Fe < Co < Ni < Cu < Zn. Fe and Co should react at room temperature, whereas Cu and Zn require elevated temperatures of up to 520 K for rapid reaction.[34] In the case of Ni, the broad range of calculated activation barriers (between 45 and 121 kJ/mol, depending on the functional used) makes it questionable whether room temperature metalation is possible or not. On the experimental side, metalation with preadsorbed Ni on Au(111) requires heating to >520 K.[20] This was taken as evidence for the formation of Ni islands, which have a low two-dimensional vapor pressure at room temperature, and the removal of Ni atoms from the islands is the rate-limiting step. This assumption is supported by other studies of porphyrin metalation with Fe on Ag(111), where formation of Fe islands at the step edges and their dissolution at elevated temperatures in the presence of a porphyrin layer was directly observed with STM.[18,35]

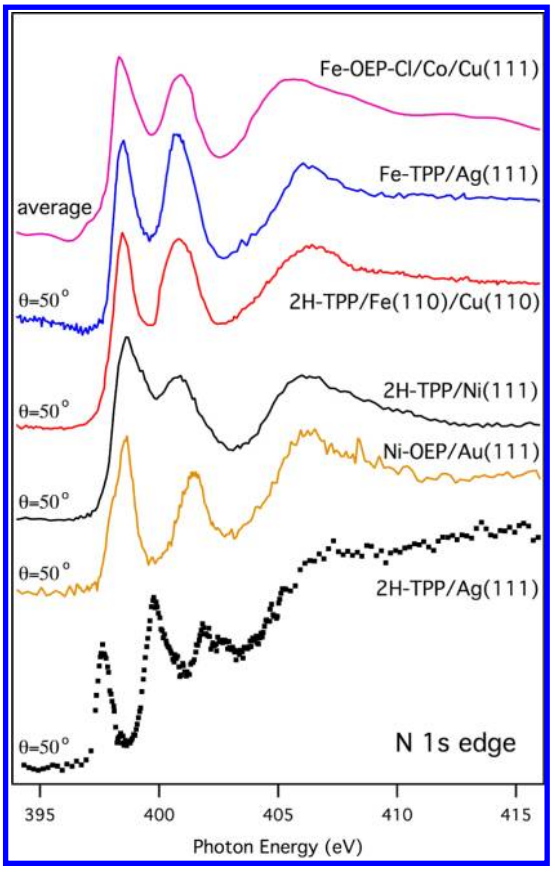

Figure 2. Single-layer N 1s NEXAFS spectra of (from top to bottom) Fe-OEP-Cl/Co/Cu(111) as measured by Wende *et al.*,[33] of metalated Fe-TPP on Ag(111),[21] our data of 2H-TPP monolayer on Fe(110)/Cu(110) and on Ni(111), forming the corresponding Fe-TPP and Ni-TPP layers, respectively, Ni-OEP deposited on Au(111),[32] and 2H-TPP deposited at room temperature on Ag(111). The angle between the linear polarization and the surface plane is shown. The spectrum of Wende *et al.* is a linear combination of the two angles reported in ref 33.

Our experimental study shows that all N atoms are equivalent, so the macrocycle redox reaction indeed occurs at room temperature for Fe(110) and Ni(111). We propose that the reaction is due to the inclusion in the macrocycle of a surface metal atom since a similar behavior was observed by Raval and co-workers[24,27] on Cu(110), where copper adatoms were weakly attracted to adsorbed free-base porphyrins at specific molecular sites after annealing above 380 K, and by Gonzalez-Moreno *et al.*,[26] where protoporphyrins on Cu(100) and, in particular, on Cu(110) surfaces seem to melalate by Cu surface atoms at room temperature. In these last cases, however, the porphyrins have small chain groups as meso-substituents, so the macrocycle is allowed to go very close to the substrate atoms, while in our case the distance is quite large due to the presence of rotated phenyl groups. In fact, the presence of phenyl surfaces tilted by an average angle of 30−35° with respect to the substrate surfaces and the macrocycle having mainly flat adsorption geometry with a saddle shape configuration (distortion angle of

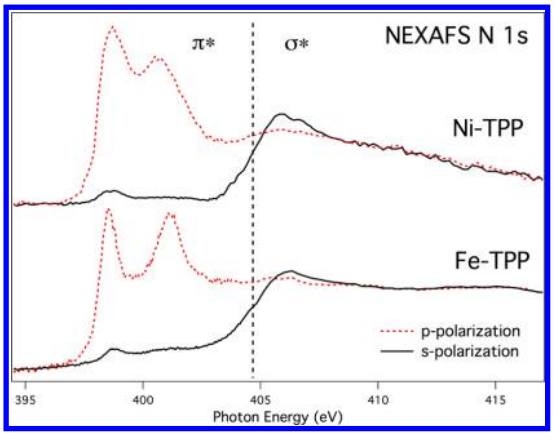

Figure 3. NEXAFS spectra at the N 1s threshold as a function of the linear polarization incidence angle of the light with respect to the surface plane; p-polarization indicates a situation where the linear polarization is perpendicular to the surface, and s-polarization means that the linear polarization is parallel to the surface plane.

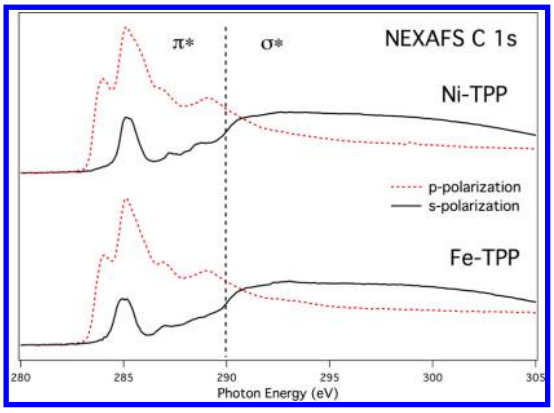

Figure 4. NEXAFS spectra at the C 1s threshold as a function of the linear polarization incidence angle of the light with respect to the surface plane; p-polarization indicates a situation where the linear polarization is perpendicular to the surface, and s-polarization means that the linear polarization is parallel to the surface plane.

the pyrrole rings of about 18°) on both Fe(110) and Ni(111) can be obtained looking at the dichroism in the NEXAFS resonances at the N 1s and C 1s thresholds as a function of the light linear polarization. Figures 3 and 4 show the comparison between NEXAFS spectra in p-polarization (linear light polarization close to the surface plane perpendicular) and s-polarization (linear light polarization in the surface plane) for 2H-TPP on Ni(111) and Fe(110) at the N 1s and C 1s threshold, respectively. From N 1s spectra, it is clear that the macrocycle is almost parallel to the surface plane with the π^* resonaces almost lost in s-polarization. Anyway, a small intensity is still visible in both Ni(111) and Fe(110) substrates, indicating a slightly distortion of the macrocycle. This distortion is also visible at the C 1s threshold on Ni(111), where the first π^* peak (~284 eV) that belongs to the carbon atoms of the macrocycle[36] remains partly visible also in the s-polarization spectra, while it disappears in the spectra of 2H-TPP of Fe(110). The average tilt angle of the nitrogen π^* states with respect to the surface normal of about 18° for both substrates can be obtained using the Stöhr formula for three or more domains,[37] while the carbon π^* states (~284 eV) of the macrocycle seem to have a similar tilt angle on Ni(111) remaining, instead, more perpendicular to the substrate surface on Fe(110). The most intense feature in the C 1s spectra at about 285 eV mainly belongs to the excitation of π^* states of phenyl rings.[36] Although we observe a huge dichroism, the intensity remains quite high also in s-polarization. The area ratio of this feature between the s-polarization and the p-polarization is 0.31 for Fe(110) and 0.38 for Ni(111). According to the Stöhr formula for three or more domains,[37] average adsorption angles for the phenyl ring surface (with respect to the substrate surface plane) close to 30° for Fe(110) and 35° for Ni(111) are obtained.

More recently, new experimental evidence of metalation of 2H-TPP on Cu(111) was provided by Diller *et al.*,[28] but just after annealing at about 420 K, which is probably related to the room temperature adsorption conformation of 2H-TPP, as suggested by Buchner and co-workers.[29]

To confirm the experimental evidence and to understand whether the metal atom incorporated in the macrocycle is more likely to derive from surface adatoms or from a surface vacancy created by the molecule, we performed large-scale *ab initio* calculations based on density functional theory (see Experimental Section for details). Given the computational cost necessary for large systems, we restricted our investigation to the more critical system 2H-TPP/Ni(111) because, according to calculations[34] and experimental evidence,[20] adding a Ni ion in the macrocycle should require annealing above 520 K, while for Fe ions, the reaction may happen also at room temperature. Despite the evidence from the literature that a considerable energy gain corresponds to 3d-metal atom inclusion into a free isolated 2H-TPP molecule when the source of metal atoms is constituted by isolated atoms,[34,35] it is not obvious that such a reaction would be exothermic when occurring on a metallic substrate: on one side, the chemical potential of the metal atom at the surface is considerably lower compared to the isolated atom case (the highest possible value), on the other case, molecular rearrangements, in order to include the atom, will have to compete with van der Waals forces.

We computed different adsorption geometries for a 2H-TPP molecule on a Ni(111) surface and found that the energies of the different minima lay within 0.2 eV of each another. Starting from the lowest energy configuration that we found, we computed the energy difference between a configuration where a Ni adatom stays on the Ni(111) surface far from the adsorbed molecule and one where the metal atom is incorporated in the molecule with a consequent release of a H_2

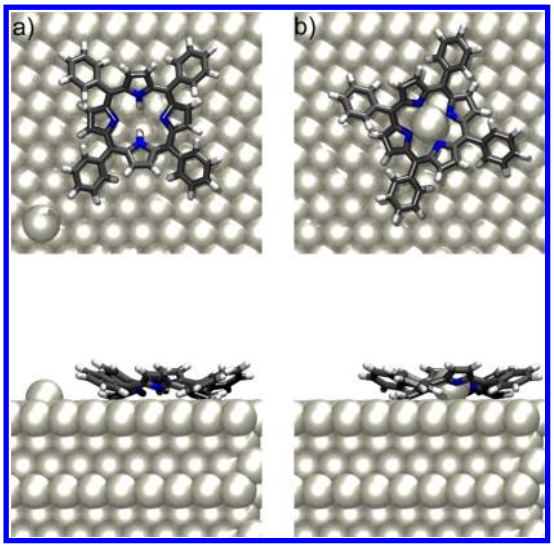

Figure 5. Top view (top) and side view (bottom) of the equilibrium geometries for the 2H-TPP molecule adsorbed on Ni(111) in the presence of a Ni adatom (a) and in the case of incorporating the Ni adatom (b). The energy gain upon embedding the Ni adatom in the macrocycle is 0.89 eV.

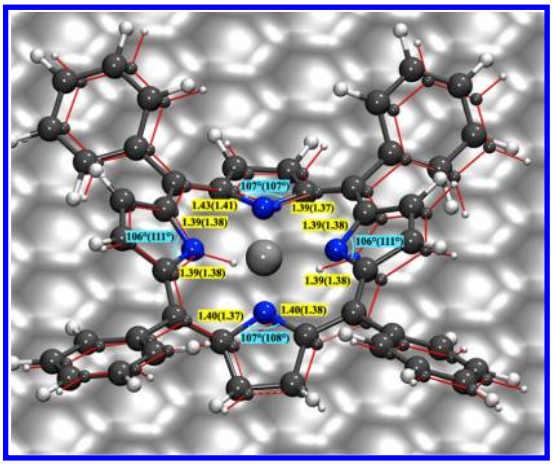

Figure 6. Structural modifications from DFT optimization of a 2H-TPP molecule upon dehydrogenation and inclusion of a Ni adatom in the macrocycle. The latter results at a bridge site on the Ni(111), at a distance of 3 Å from the first Ni neighbors of the substrate. In the figure, the red frame with small atom balls represents the original structure; the bold colored frame with larger atom balls depicts instead the optimized metalated structure. The numbers indicate the C−N−C angles and the C−N bond distances in the metalated (nonmetalated) structure.

molecule in vacuum (see Figure 5). Our results indicate that the inclusion of Ni adatoms is thermodynamically favored by 0.89 eV.

We show in Figure 6 the structural modifications upon metalation of the 2H-TPP molecule as obtained from the DFT optimization. We observe that the four nitrogen atoms have a distance from the central Ni atom of 1.94 Å. The dehydrogenation does not modify the C−N bond distances considerably but slightly decreases the C−N−C angle from 111° (in the pyrrolic configuration) to 106°. After metalation, the C−N−C angles in the four iminic units are thus equivalent at the value of 106/107°. The buckling of the molecule orthogonally to the surface (about 2.6 Å not considering the hydrogens) is not modified upon metalation. The distance of the central Ni atom, showing a bridge position on the Ni(111) surface, from the two nearest neighbors in the substrate, amounts to 3 Å. Both in the metalated and nonmetalated structure, the molecule has a saddle shape, with the pyrrolic units pointing down toward the center. The phenyl rings are rotated with an angle of about 40° with respect to the surface, in both molecular configurations, in quite good agreement with the 35° obtained in the experimental data. The obtained rotations of the iminic units (18° before and 17° after metalation) and pyrrolic units (30° before metalation and 29° after metalation) are slightly larger than the average angle extracted from the experiments (18°). The N surface distance ranges from 2.5 Å (pyrrolic N atoms) to 3.1 Å (iminic N atoms).

We then considered the hypothesis that the 2H-TPP molecule is able to create a Ni vacancy at the surface to embed the metal atom. In this case, the process is not thermodynamically favored and corresponds to an energy loss of 0.69 eV (a relatively small value) if the vacancy is static. We thus conclude that the final configuration with an intact substrate and a Ni atom included in the molecule is thermodynamically most favored. Nothing can be said *a priori* about the reaction mechanism: the calculation of the reaction rates would require the study of all of the most probable reaction paths. The relatively small energy loss of 0.69 eV corresponding to the promotion of a substrate atom to the macrocycle center, with vacancy creation, suggests however that this process could be an intermediate step of a concerted mechanism of reaction. The latter could have a lower overall reaction barrier with respect to the simpler and direct adatom migration "beneath" the molecule.

Recent studies for 2H-TPP adsorption on Cu(111) have shown the tendency of iminic nitrogens to bind to surface atoms even in a strong fashion.[28,29] Conversely, no such evidence is present for Au(111) or Ag(111) adsorption. To test this possibility in our case, we searched for a new set of possible configurations starting from a geometry where iminic N atoms point toward the surface and pyrrolic rings are, as a consequence, tilted in the opposite direction. We were able to find a new state, considerably more stable (5.8 eV) compared to the geometries already discussed. Remarkably, in this state, the phenyl rings are flat as well as the distorted pyrrolic groups, whereas two strong chemical bonds are formed between the upright iminic groups and a Ni surface atom. This, together with a stronger bonding of the phenyl-C atoms to the surface, causes a huge gain in energy.

However, the geometry that we reach is not compatible with the experimental findings, neither something of this kind, with flat phenyl rings and upright iminic

groups, has ever been observed experimentally. Indeed, such a structure would give completely different XPS and NEXAFS spectra and, at variance with the proposed pristine geometry with the pyrrolic units slightly pointing to the surface, would lose 0.38 eV upon adatom diffusion-based metalation. Another important contrast to the experiment concerns the flat orientation of the phenyl rings (see Supporting Information, Figure S3).

CONCLUSION

Using high-resolution X-ray spectroscopy and density functional theory calculations, we have shown that 2*H*-tetraphenyl porphyrins metalate at room temperature by incorporating a surface metal atom when a (sub)monolayer is deposited on 3d magnetic substrates, such as Fe(110) and Ni(111). For the most critical case, Ni(111), the calculations demonstrate that the redox metalation reaction would be exothermic with an energy gain of 0.89 eV upon embedding a Ni adatom in the macrocycle. This attactive interaction with substrate atoms enables the formation of metallo-organic complexes, simplifying the synthesis of the metalation process and certainly improving the interaction with the substrate. We believe that the described reaction should be relevant for chemisorption of different free-base macrocyclic molecules on other reactive surfaces. The achievement of a complete metalation by Fe and Ni can be regarded as a test case for a successful preparation of spintronic devices by means of molecular-based magnets (orgamometallic nanostructures) and inorganic magnetic substrates.

EXPERIMENTAL SECTION

Experiments were carried out at the BACH[38] and ALOISA[39] beamlines of the Elettra synchrotron radiation facility in Trieste. The metal substrates, Ni(111) and Cu(110), were cleaned by Ar^+ sputtering at 1 keV and annealing at 700 °C. Fe layers on a clean Cu(110) surface were deposited using a Omicron e-beam evaporator until no Cu signals were visible by photoemission (about 15 ML). Under these conditions, we obtain ordered rough Fe films on Cu(110) in the face-centered cubic structure with the (110) face on top.[40] 2H-TPP molecules were deposited on the substrates kept at room temperature from a homemade tantalum basket heated by current flow at 570 K. The monolayer was defined as the maximum surface coverage after the sublimation of a deposited multilayer at 570 K, and the relative intensities of C 1s and N 1s photoemission core level peaks with respect to the substrate peaks were taken as reference for the deposition of (sub)monolayer at room temperature. The samples were characterized by photoemission, low-energy electron diffraction, reflection high-energy electron diffraction, and X-ray absorption spectroscopy measurements. The energy resolution for photoemission and X-ray absorption spectroscopy was better than 150 meV. Photoelectrons were collected using a hemispherical electron energy analyzer. Binding and photon energies were calibrated by means of the metal Fermi level in photoemission and by measuring the absorption spectrum of reference samples. Ultrahigh vacuum (UHV) conditions (in the pressure range of 10^{-10} mbar) were maintained throughout the experiment.

Photon energies of 550 and 400 eV were used for N 1s and C 1s XPS measurements (not shown), respectively. Near-edge X-ray absorption fine structure (NEXAFS) spectroscopy was measured both in Auger and partial electron yield modes, while scanning the photon energy across the C and N *K*-edges. The orientation of the surface with respect to the linear polarization of the synchrotron beam was changed by rotating (θ angle) the sample around the beam axis while keeping a constant grazing incident angle of 6°. This scattering geometry allows one to change from linear s-polarization at $\theta = 0°$ to p-polarization at $\theta = 90°$ without variation of the illuminated area on the sample. The raw data were normalized to the total photon flux measured at the same time with the NEXAFS spectrum and divided by the NEXAFS spectrum of the clean substrate taken at the same threshold.[41] The total error on the extracted molecular adsorption angles, considering the above normalization procedure and the chosen angular step of 5°, is ±3°. The NEXAFS data shown in Figure 2 were taken at $\theta = 50°$ close to the magic angle at which every resonance appears in the spectrum independently on the orientation of the corresponding orbital.

The *ab initio* simulations were performed within the mixed Gaussian and plane wave method implemented in the cp2k code.[42] Atomic species were represented *via* pseudopotentials of the Goedecker type,[43] and gradient corrections as parametrized within the revPBE[44] approximation were employed for the exchange correlation functional. In order to account for the van der Waals interactions, we used the empirical scheme proposed by Grimme ("DFT-D3" version).[45] To model 2H-TPP adsorbed on Ni(111), we used the repeated slab geometry:[46] a fully periodic large simulation cell with dimensions of 22.7 × 21.9 Å^2 (corresponding 9 × 5 Ni(111) rectangular cells) contained six layers of Ni, the molecule, and additional 20 Å of vacuum. The energy for equilibrium geometries was obtained with a geometry optimization procedure iterated until forces on the atoms were lower than 0.5×10^{-4} au. Two Ni(111) atomic layers were fixed to bulk positions, and all remaining atoms were allowed to move.

Conflict of Interest: The authors declare no competing financial interest.

Acknowledgment. This work was supported by MIUR under the PRIN/COFIN Contract 20087NX9Y7 and FIRB Projects RBAP11C58Y and RBFR10DAK6. The Swiss National Science Foundation (Project 200020-132375) and the computational time from the Swiss Supercomputing Center (CSCS) are also acknowledged. We thank M. Pedio for providing us the unpublished data on Ni-OEP.

Supporting Information Available: XPS study of the Rh and Mn metalation as well as calculations and discussion for another adsorption geometry of 2H-TPP on Ni(111). This material is available free of charge *via* the Internet at http://pubs.acs.org.

REFERENCES AND NOTES

1. Forrest, S. R. Ultrathin Organic Films Grown by Organic Molecular Beam Deposition and Related Techniques. *Chem. Rev.* **1997**, *97*, 1793–1896.
2. Lehn, J.-M. Toward Self-Organization and Complex Matter. *Science* **2002**, *295*, 2400–2403.
3. Bonifazi, D.; Enger, O.; Diederich, F. Supramolecular C_{60} Fullerene Chemistry on Surfaces. *Chem. Soc. Rev.* **2007**, *36*, 390–414.
4. Gliemann, H.; Wöll, C. Epitaxially Grown Metal-Organic Frameworks. *Mater. Today* **2012**, *15*, 110–116.
5. Hoeben, F. J. M.; Jonkheijm, P.; Meijer, E. W.; Schenning, A. P. H. J. About Supramolecular Assemblies of π-Conjugated Systems. *Chem. Rev.* **2005**, *105*, 1491–1546.
6. Yoshimoto, S.; Itaya, K. Advances in Supramolecularly Assembled Nanostructures of Fullerenes and Porphyrins at Surfaces. *J. Porphyrins Phthalocyanines* **2007**, *11*, 313–333.

7. Gottfried, J. M.; Marbach, H. Surface-Confined Coordination Chemistry with Porphyrins and Phthalocyanines: Aspects of Formation, Electronic Structure, and Reactivity. *Z. Phys. Chem.* **2009**, *223*, 53–74.
8. Guillaud, G.; Simon, J.; Germain, J. P. Metallophthalocyanines Gas Sensors, Resistors and Field Effect Transistors. *Coord. Chem. Rev.* **1998**, *178*−*180*, 1433–1484.
9. Guldi, D. M. Fullerene-Porphyrin Architectures; Photosynthetic Antenna and Reaction Center Models. *Chem. Soc. Rev.* **2002**, *31*, 22–36.
10. Imahori, H.; Fukuzumi, S. Porphyrin- and Fullerene-Based Molecular Photovoltaic Devices. *Adv. Funct. Mater.* **2004**, *14*, 525–536.
11. Hulsken, B.; Van Hameren, R.; Gerritsen, J. W.; Khoury, T.; Thordarson, P.; Crossley, M. J.; Rowan, A. E.; Nolte, R. J. M.; Elemans, J. A. A. W.; Speller, S. Real-Time Single-Molecule Imaging of Oxidation Catalysis at a Liquid−Solid Interface. *Nat. Nanotechnol.* **2007**, *2*, 285–289.
12. Scheybal, A.; Ramsvik, T.; Bertschinger, R.; Putero, M.; Nolting, F.; Jung, T. A. Induced Magnetic Ordering in a Molecular Monolayer. *Chem. Phys. Lett.* **2005**, *411*, 214–220.
13. Auwärter, W.; Weber-Bargioni, A.; Brink, S.; Riemann, A.; Schiffrin, A.; Ruben, M.; Barth, J. V. Controlled Metalation of Self-Assembled Porphyrin Nanoarrays in Two Dimensions. *ChemPhysChem* **2007**, *8*, 250–254.
14. Buchner, F.; Schwald, V.; Comanici, K.; Steinruck, H.-P.; Marbach, H. Microscopic Evidence of the Metalation of a Free-Base Porphyrin Monolayer with Iron. *ChemPhysChem* **2007**, *8*, 241–243.
15. Kretschmann, A.; Walz, M.; Flechtner, K.; Steinruck, H.-P.; Gottfried, J. M. Tetraphenylporphyrin Picks up Zinc Atoms from a Silver Surface. *Chem. Commun.* **2007**, 568–570.
16. Gottfried, J. M.; Flechtner, K.; Kretschmann, A.; Lukasczyk, T.; Steinruck, H.-P. Direct Synthesis of a Metalloporphyrin Complex on a Surface. *J. Am. Chem. Soc.* **2006**, *128*, 5644–5645.
17. Bai, Y.; Buchner, F.; Kellner, I.; Schmid, M.; Vollnhals, F.; Steinruck, H.-P.; Marbach, H.; Gottfried, J. M. Adsorption of Cobalt(II) Octaethylporphyrin and 2*H*-Octaethylporphyrin on Ag(111): New Insight into the Surface Coordinative Bond. *New J. Phys.* **2009**, *11*, 125004.
18. Buchner, F.; Flechtner, K.; Bai, Y.; Zillner, E.; Kellner, I.; Steinruck, H.-P.; Marbach, H.; Gottfried, J. M. Coordination of Iron Atoms by Tetraphenylporphyrin Monolayers and Multilayers on Ag(111) and Formation of Iron-Tetraphenylporphyrin. *J. Phys. Chem. C* **2008**, *112*, 15458–15465.
19. Weber-Bargioni, A.; Reichert, J.; Seitsonen, A. P.; Auwärter, W.; Schiffrin, A.; Barth, J. V. Interaction of Cerium Atoms with Surface-Anchored Porphyrin Molecules. *J. Phys. Chem. C* **2008**, *112*, 3453–3455.
20. Chen, M.; Feng, X.; Zhang, L.; Ju, H.; Xu, Q.; Zhu, J.; Gottfried, J. M.; Ibrahim, K.; Qian, H.; Wang, J. Direct Synthesis of Nickel(II) Tetraphenylporphyrin and Its Interaction with a Au(111) Surface: A Comprehensive Study. *J. Phys. Chem. C* **2010**, *114*, 9908–9916.
21. Di Santo, G.; Castellarin-Cudia, C.; Fanetti, M.; Taleatu, B.; Borghetti, P.; Sangaletti, L.; Floreano, L.; Magnano, E.; Bondino, F.; Goldoni, A. Conformational Adaptation and Electronic Structure of 2*H*-Tetraphenylporphyrin on Ag(111) during Fe Metalation. *J. Phys. Chem. C* **2011**, *115*, 4155–4162.
22. Li, Y.; Xiao, J.; Shubina, T. E.; Chen, M.; Shi, Z.; Schmid, M.; Steinrück, H.-P.; Gottfried, J. M.; Lin, N. Coordination and Metalation Bifunctionality of Cu with 5,10,15,20-Tetra(4-pyridyl)porphyrin: Toward a Mixed-Valence Two-Dimensional Coordination Network. *J. Am. Chem. Soc.* **2012**, *134*, 6401–6408.
23. Hanke, F.; Haq, S.; Raval, R.; Persson, M. Heat-to-Connect: Surface Commensurability Directs Organometallic One-Dimensional Self-Assembly. *ACS Nano* **2011**, *5*, 9093–9103.
24. Haq, S.; Hanke, F.; Dyer, M. S.; Persson, M.; Iavicoli, P.; Amabilino, D. B.; Raval, R. Clean Coupling of Unfunctionalized Porphyrins at Surfaces To Give Highly Oriented Organometallic Oligomers. *J. Am. Chem. Soc.* **2011**, *133*, 12031–12039.
25. Di Santo, G.; Blankenburg, S.; Castellarin-Cudia, C.; Fanetti, M.; Borghetti, P.; Sangaletti, L.; Floreano, L.; Verdini, A.; Magnano, E.; Bondino, F.; *et al.* Supramolecular Engineering through Temperature-Induced Chemical Modification of 2*H*-Tetraphenylporphyrin on Ag(111): Flat Phenyl Conformation and Possible Dehydrogenation Reactions. *Chem.—Eur. J.* **2011**, *17*, 14354–14359.
26. Gonzales-Moreno, R.; Sanchez-Sanchez, C.; Trelka, M.; Otero, R.; Cossaro, A.; Verdini, A.; Floreano, L.; Ruiz-Bermejo, M.; García-Lekue, A.; Martín-Gago, J. A.; *et al.* Following the Metalation Process of Protoporphyrin IX with Metal Substrate Atoms at Room Temperature. *J. Phys. Chem. C* **2011**, *115*, 6849–6854.
27. Dyer, M. S.; Robin, A.; Haq, S.; Raval, R.; Persson, M.; Klimes, J. Understanding the Interaction of the Porphyrin Macrocycle to Reactive Metal Substrates: Structure, Bonding, and Adatom Capture. *ACS Nano* **2011**, *5*, 1831–1838.
28. Diller, K.; Klappenberger, F.; Marschall, M.; Hermann, K.; Nefedov, A.; Wöll, Ch.; Barth, J. V. Self-Metalation of 2*H*-Tetraphenylporphyrin on Cu(111): An X-ray Spectroscopy Study. *J. Chem. Phys.* **2012**, *136*, 014705.
29. Buchner, F.; Xiao, J.; Zillner, E.; Chen, M.; Röckert, M.; Ditze, S.; Stark, M.; Steinruck, H.-P.; Gottfried, J. M.; Marbach, H. Diffusion, Rotation, and Surface Chemical Bond of Individual 2*H*-Tetraphenylporphyrin Molecules on Cu(111). *J. Phys. Chem. C* **2011**, *115*, 24172–24177.
30. Anderson, H. L. Building Molecular Wires from the Colours of Life: Conjugated Porphyrin Oligomers. *Chem. Commun.* **1999**, 2323–2330.
31. Hieringer, W.; Flechtner, K.; Kretschmann, A.; Seufert, K.; Auwärter, W.; Barth, J. V.; Görling, A.; Gottfried, J. M. The Surface Trans Effect: Influence of Axial Ligands on the Surface Chemical Bonds of Adsorbed Metalloporphyrins. *J. Am. Chem. Soc.* **2011**, *133*, 6206–6222.
32. Pedio, M. Private communication.
33. Wende, H.; Bernien, M.; Luo, J.; Sorg, C.; Ponpandian, N.; Kurde, J.; Miguel, J.; Piantek, M.; Xu, X.; Eckhold, Ph.; *et al.* Substrate-Induced Magnetic Ordering and Switching of Iron Porphyrin Molecules. *Nat. Mater.* **2007**, *6*, 516–520.
34. Shubina, T. E.; Marbach, H.; Flechtner, K.; Kretschmann, A.; Jux, N.; Buchner, F.; Steinrück, H.-P.; Clark, T.; Gottfried, J. M. Principle and Mechanism of Direct Porphyrin Metalation: Joint Experimental and Theoretical Investigation. *J. Am. Chem. Soc.* **2007**, *129*, 9476–9483.
35. Buchner, F.; Kellner, I.; Steinruck, H. P.; Marbach, H. Modification of the Growth of Iron on Ag(111) by Predeposited Organic Monolayers. *Z. Phys. Chem.* **2009**, *223*, 131–144.
36. Castellarin-Cudia, C.; Vilmercati, P.; Larciprete, R.; Cepek, C.; Zampieri, G.; Verdini, A.; Cossaro, A.; Floreano, L.; Morgante, A.; Sangaletti, L.; *et al.* Electronic Structure and Molecular Orientation of a Zn-Tetraphenyl-Porphyrin Multilayer on Si(111). *Surf. Sci.* **2006**, *600*, 4013–4018.
37. Stöhr, J. *NEXAFS Spectroscopy*; Gomer, R., Ed.; Springer-Verlag: Berlin, 1992.
38. Zangrando, M.; Finazzi, M.; Paolucci, G.; Comelli, G.; Diviacco, B.; Walker, R. P.; Cocco, D.; Parmigiani, F. BACH, the Beamline for Advanced Dichroic and Scattering Experiments at ELETTRA. *Rev. Sci. Instrum.* **2001**, *72*, 1313–1319.
39. Floreano, L.; Naletto, G.; Cvetko, D.; Gotter, R.; Malvezzi, M.; Marassi, L.; Morgante, A.; Santaniello, A.; Verdini, A.; Tommasini, F.; *et al.* Performance of the Grating-Crystal Monochromator of the ALOISA Beamline at the Elettra Synchrotron. *Rev. Sci. Instrum.* **1999**, *70*, 3855–3864.
40. Tian, D.; Jona, F.; Marcus, P. M. Structure of Ultrathin Films of Fe on Cu{111} and Cu{110}. *Phys. Rev. B* **1992**, *45*, 11216–11221.
41. Floreano, L.; Cossaro, A.; Gotter, R.; Verdini, A.; Bavdek, G.; Evangelista, F.; Ruocco, A.; Morgante, A.; Cvetko, D. Periodic Arrays of Cu-Phthalocyanine Chains on Au(110). *J. Phys. Chem. C* **2008**, *112*, 10794–10802.
42. VandeVondele, J.; Krack, M.; Mohamed, F.; Parrinello, M.; Chassaing, T.; Hutter, J. Quickstep: Fast and Accurate Density Functional Calculations Using a Mixed Gaussian

and Plane Waves Approach. *Comput. Phys. Commun.* **2005**, *167*, 103–128http://cp2k.berlios.de.
43. Goedecker, S.; Teter, M.; Hutter, J. Separable Dual-Space Gaussian Pseudopotentials. *Phys. Rev. B* **1996**, *54*, 1703–1710.
44. Zhang, Y.; Yang, W. Comment on "Generalized Gradient Approximation Made Simple". *Phys. Rev. Lett.* **1998**, *80*, 890–893.
45. Grimme, S.; Antony, J.; Ehrlich, S.; Krieg, H. A Consistent and Accurate *Ab-Initio* Parametrization of Density Functional Dispersion Correction (DFT-D) for the 94 Elements H-Pu. *J. Chem. Phys.* **2010**, *132*, 154104.
46. Pickett, W. E. Pseudopotential Methods in Condensed Matter Applications. *Comput. Phys. Rep.* **1989**, *9*, 115–198.